


Article

Detection of Aflatoxin B₁ in Wheat Based on Nucleic Aptamer Chemiluminescence Sensor

Zebing Zhang, Caizhang Wu and Zhike Zhao * 

College of Electrical Engineering, Henan University of Technology, Zhengzhou 450001, China; zhangzebing@stu.haut.edu.cn (Z.Z.); wucaizhang@haut.edu.cn (C.W.)

* Correspondence: zhaozhike@haut.edu.cn

Abstract: In this study, we developed a low-cost, high-sensitivity chemiluminescence competitive aptamer sensor for the detection of aflatoxin B₁ (AFB₁) in wheat samples. The optical fiber sensor was self-made, and it utilized biotin and streptavidin (SA) link aptamer and horseradish peroxidase (HRP) for the chemiluminescence detection, achieving competitive assay between the AFB₁ and AFB₁ antigen. We adjusted the experimental conditions of the sensor base on the date of optimization of the experimental conditions and chose coated antigens on the surface of carboxyl magnetic particles. Under conditions optimized by testing key parameters, the assay results showed that the chemiluminescence intensity and AFB₁ concentration demonstrated a strong linear relationship ($R^2 = 0.995$), the dynamic range was from 0.1 to 10 ng/mL with a detection limit of 0.09 ng/mL, and the aptamer exhibited good specificity and anti-interference ability. Testing the wheat samples showed that the spiked recovery rate ranged from 79.19% to 113.21%. The sensor possesses characteristics of low detection limits, simple manufacturing methods, and affordability, providing a novel solution for the development of low-cost and high-sensitivity AFB₁ detection equipment.

Keywords: aflatoxin B₁ detection; aptamer; chemiluminescence sensor; optical fiber; wheat



Academic Editor: Manel del Valle

Received: 13 December 2024

Revised: 29 January 2025

Accepted: 5 February 2025

Published: 7 February 2025

Citation: Zhang, Z.; Wu, C.; Zhao, Z. Detection of Aflatoxin B₁ in Wheat Based on Nucleic Aptamer Chemiluminescence Sensor. *Sensors* **2025**, *25*, 988. <https://doi.org/10.3390/s25040988>

Copyright: © 2025 by the authors. Licensee MDPI, Basel, Switzerland. This article is an open access article distributed under the terms and conditions of the Creative Commons Attribution (CC BY) license (<https://creativecommons.org/licenses/by/4.0/>).

1. Introduction

Food security is directly related to people's quality of life and health level, so it has attracted public attention. Aflatoxin is one of the major threats to food security in the whole process of food storage. Aflatoxin has a strong pollution ability, which is easy to cause harm to grain, and this phenomenon is more serious in hot and humid areas [1,2]. The basic structure of aflatoxin is dihydrocoumarin, which is composed of difuran ring and oxynaphthalene ortho ketone. There are many kinds of aflatoxins, of which B, G, and M series are the most prominent ones, namely AFB₁, AFB₂, AFG₁, AFG₂, AFM₁, and AFM₂ [3]. Among them, AFB₁ is mainly a secondary metabolite produced by *Aspergillus flavus* and *Aspergillus parasiticus* [4,5]. Aflatoxin B₁ is widely found in peanut, corn, soybean, wheat, and other food and agricultural products [6]. When food is contaminated by AFB₁, it can enter human and animal bodies through the food chain, inhibit the synthesis of proteins; enzymes, organic substances, cellular DNA, and RNA in human and animal bodies; and then interfere with various metabolic processes, causing serious harm to human and animal health [7,8], clinical investigations have found that AFB₁ can be transformed into AFM₁, AFBO, and other harmful substances in the human body, which can cause genetic and protein expression disorders, lead to metabolic disorders, and even lead to cell distortion or cancer, causing serious damage to the human body [9]. In 1993, the Cancer Research

Institute of the World Health Organization (WHO) classified it as a class I carcinogen (for humans). The European Commission strictly stipulated that the permitted level of aflatoxin B₁ be set at $\leq 2 \mu\text{g}/\text{kg}$ in some cereals and their products $2 \mu\text{g}/\text{kg}$; the maximum limit of aflatoxin in China's current standard GB 2761-2017 is $5\text{--}20 \mu\text{g}/\text{kg}$ [10–12]. To ensure the safety of grain storage and people's health and effectively monitor aflatoxin pollution, there is an urgent need for an AFB₁ toxin detection system applied to the grain industry. At present, a variety of detection methods have been reported. Common methods are mainly large-scale instrument detection, including high-performance liquid chromatography (HPLC) [13], fluorescence (FL) [14], electrochemiluminescence (ECL) [15], photo electrochemistry (PEC) [16], surface enhanced Raman spectroscopy (SERS) [17], optical fibers etc. [18].

In recent years, an innovative based method has been developed in the field of toxin detection. Aptamer is a single-stranded oligonucleotide sequence, which is screened in vitro through the systematic evolution of ligands by exponential enrichment (SELEX), and it has the advantages of low cost, high stability, and strong specificity [19]. Compared with antibodies, aptamers have stronger tolerance to environmental changes, better stability, and advantages such as fast chemical synthesis and low cost, so aptamers are also called the “artificial antibody” [20–22]. Aptamers have a simple structure and are easy to modify. Various substances required for experiments can be added at the 5' end or 3' end. For example, Li et al. [23] designed an experimental method for the combination of aptamer and SA-HRP based on the aptamer modified with biotin and established a simple and sensitive DNA magnetic particle chemiluminescence method for the detection of avian influenza H₁N₁ virus DNA. Shim et al. [24] developed a chemiluminescence competitive aptamer assay for AFB₁ using a hemin/G-quadruplex HRP-DNAzyme linked with an aptamer specific to AFB₁. Yao et al. [25] developed a chemiluminescence aptamer sensor based on the HRP-catalyzed chemiluminescence reaction of luminol. They used a mixed chain reaction (HCR) signal amplification strategy to improve detection sensitivity and employed magnetic separation techniques to further reduce background signals. In 2022, Hu et al. and others used multimode optical fiber combined with an optical fiber photon counting probe to detect the target signal and designed an aflatoxin B₁ optical fiber detection system based on photoelectric detection technology [26].

The conventional detection method coats the antigen on the microplate, the separation performance of the microplate is weak, and the steps are cumbersome, while the large surface area to volume ratio of the magnetic particles increases the enrichment of the material on its surface and improves the separation efficiency. Modification of carboxyl, amino, thiol, and other active groups on the surface of magnetic particles can provide a wide choice for the enrichment of different target substances. Therefore, new research began to use magnetic particles combined with aptamers, use the superparamagnetism of magnetic particles, use magnetic particles to separate and purify target substances from various complex substances, strengthen the separation performance of the experiment, and omit centrifugation and other operations. In 2023, Lu et al. [27] developed a method for detecting aflatoxin B₁ (AFB₁) in plant protein meat by SERS aptamer sensor composed of magnetic nanoparticles of ferro-tetroxide.

To reduce the cost of sensor development and improve the sensitivity of the sensor, we designed a novel aptamer chemiluminescence sensor based on the aptamer. In this work, we investigated the uses of biotin, SA-HRP, and Luminol. And we examined the optimization of experimental conditions, specificity, and anti-interference ability; assessed the efficiency of the developed assay included its use for AFB₁ detection in wheat samples, and compared the sensors with similar methods.

2. Materials and Methods

2.1. Materials and Reagents

AFB₁-related mycotoxins (AFB₂, AFG₁, and ochratoxin A (OTA)), bovine serum albumin (BSA), Luminol, streptavidin conjugated with horseradish peroxidase (SA-HRP), P-iodophenol (PIP), TE buffer, 1× solution (low EDTA), phosphate buffer (PBS) (pH 7.4), methanol, H₂O₂, sodium N-hydroxy succinimide (NHS), 1-(3-dimethylaminopropyl)-3-ethylcarbodiimide (EDC), and Tween 20 were purchased from Sangon Biotech. Co., Ltd. (Shanghai, China). Ultrapure water for experiment was purchased from Ruixi chemical treatment plant (Jiaxing, China); aflatoxin B₁ antigen (AFB₁-OVA) was purchased from Anti Biological Technology Co., Ltd. (Shenzhen, China); carboxy magnetic particles (2 μm) were purchased from Suzhou Beaver Biosciences Inc. (Suzhou, China); wheat samples were purchased from local farmers' market (Zhengzhou, China). The DNA sequences were synthesized by Sangon Biotech. Co., Ltd.; (Shanghai, China) and purified using high-performance liquid chromatography (HPLC). The DNA sequences are as follows:

GTTGGGCACGTGTTGTCTCTCTGTGTCTCGTGCCCTTCGCTAGGCCACACA; from the 5' end to the 3' end, the 5' end is modified with biotin.

2.2. Preparation of AFB₁ Standard Solution and AFB₁-Spiked Wheat Samples

We prepared AFB₁ standard solution at different concentrations (0, 0.1, 0.3, 1, 3, and 10 ng/mL) in methanol/water (10:90, *v/v*). The cross-reactivity of AFB₁-related compounds (AFB₂, AFG₁, and OTA) was also determined, with each compound prepared at a concentration of 10 ng/mL in methanol/water (10:90, *v/v*).

First, 20.0 g of wheat sample was weighted and crushed into powder, and 1.0 g of wheat flour sample was placed in a 50 mL centrifuge tube. Next, 25 mL of methanol/water (70:30, *v/v*) was added into the centrifuge tube for 20 min oscillation extraction and centrifuged for 5 min at 12,000 R/min. Then, 30 μL of supernatant were dried and mixed with 100 μL of PBS (pH 7.4), soaked for 3 min, and mixed for 20 times to obtain the sample detection solution; the obtained sample solutions (0, 0.5, 1, 2, 5, and 10 μg/kg) were stored at 4 °C for future use [28,29].

2.3. AFB₁-OVA Coated

Next, 50 μL of the carboxyl magnetic particle solution with a concentration of 10 mg/mL was placed in a centrifuge tube, vortexed, and mixed for 10 s. It was placed on a magnetic separation rack for magnetic separation for 3 min, and the supernatant was removed. Then, 100 μL of EDC (10 mg/mL) and 100 μL of NHS (10 mg/mL) were added to the new configuration and activated at 25 °C for 20 min, and 25 ng of AFB₁-OVA antigen in 100 μL PBS were added to the magnetic particle solution and incubated at 37 °C for 1 h. After washing three times with PBST (pH 7.4, containing 0.1% Tween 20), the magnetic particle solution was blocked with 200 μL 1% BSA and kept overnight at 4 °C, and then, it was washed four times with PBST (pH 7.4, containing 0.1% Tween 20).

2.4. Chemiluminescence Competitive Aptamer Assay

We prepared an aptamer solution in TE buffer solution for later use. Then, 100 μL of aflatoxin B₁ (AFB₁) standard solution or 100 μL of AFB₁ sample solution and 100 μL of aptamer solution (0.6 nM) were added to a centrifuge tube and incubated at 30 °C for 15 min for competitive steps. After completion, we placed the magnetic particle solution on a magnetic separation rack for magnetic separation for 3 min and washed 10 times with PBST (pH 7.4, containing 0.1% Tween 20).

After the binding step between the aptamer and aflatoxin AFB₁ was completed, 100 μL of PBST (pH 7.4, containing 0.1% Tween 20) mixed solution containing 200 ng/mL SA-HRP

was added to each centrifuge tube, and the reaction was gently shaken at 37 °C for 30 min. After the reaction was complete, we placed the magnetic particle solution on a magnetic separation rack for magnetic separation for 3 min, washed it 5 times with PBST (pH 7.4, containing 0.1%, Tween 20), and washed it once with PBS (pH 7.4). The mixed solution of magnetic particle aptamers obtained after completing the binding reaction was transferred to a CL reaction tube and the washing buffer removed.

Then, 200 μL of CL reaction solution (2 mM luminol, 0.5 mM P-iodophenol (PIP), and 2 mM H_2O_2) was added to a centrifuge tube in a PBS (pH 7.4) environment. Finally, optical fibers were used to detect solutions in centrifuge tube, and the CL intensity was measured using a sensor.

3. Results

3.1. Principle of Sensor for AFB₁ Detection

A detailed depiction of AFB₁ detection is presented in Figure 1: (A) Firstly, NHS and EDC reagent are added to the magnetic particle solution to activate the magnetic particles. After that, AFB₁-OVA is coated on the magnetic particles. (B) Following this, the aptamer and AFB₁ are added to the solution and a competitive step between AFB₁ and AFB₁-OVA will start. After the competition is completed, part of the aptamer will bind to AFB₁-OVA and form the OVA-AFB₁-aptamer conjugate, and this part will be immobilized on the magnetic particle. Another part of the aptamer will bind to the free AFB₁ and form the OVA-AFB₁-aptamer conjugate. These two components, the OVA-AFB₁-aptamer conjugate and AFB₁-aptamer conjugate, are separated by magnetic force, and then, the AFB₁-aptamer conjugate in the supernatant is removed. Afterwards, SA-HRP is added to the solution, and SA-HRP binds to the aptamer through biotin on the aptamer, forming the OVA-AFB₁-aptamer-SA-HRP conjugate. Lastly, we add the CL reaction solution (luminol, P-iodophenol (PIP), and H_2O_2). The CL solution will release energy in the form of blue shimmer radiation [30] and also will detect chemiluminescence intensity with the sensor.

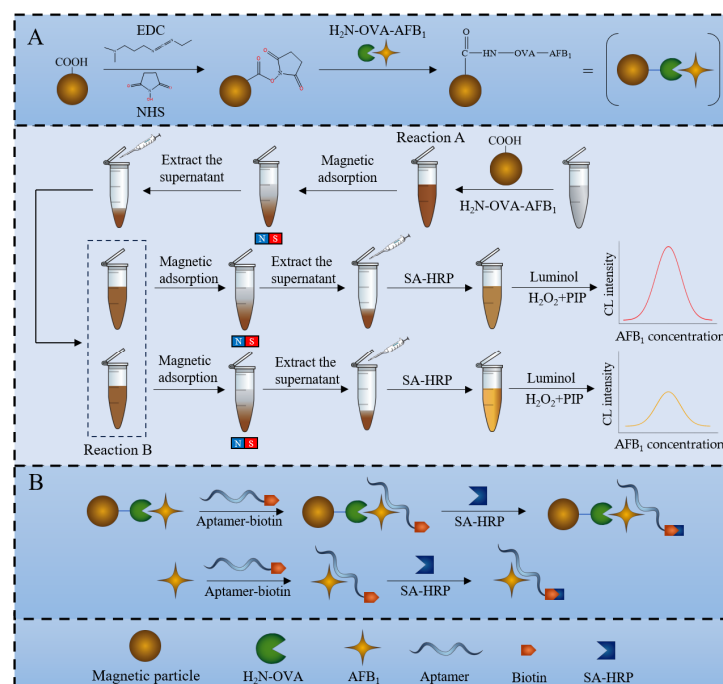


Figure 1. Schematic illustration of AFB₁ detection using the chemiluminescence sensor. (A) The process of coating antigen on magnetic particles. (B) Competitive binding aptamer mechanism between AFB₁ and AFB₁-OVA.

The experiment is based on indirect competition law, and the concentration of AFB₁ was determined by detecting the number of magnetic particle–antigen–aptamer complexes. When the concentration of AFB₁ is high, the aptamer will be more inclined to bind to the free AFB₁ and be cleared out of the test tube with the supernatant. On the contrary, the aptamer will be more inclined to bind with AFB₁ antigen and immobilize it together with the antigen on magnetic particles. When SA-HRP is added, and the AFB₁ concentration is high, more aptamers will be cleared out of the test tube with AFB₁, reducing the chance of SA-HRP binding to aptamers. The SA-HRP fixed on magnetic particles will decrease, and the chemiluminescence intensity will also weaken. On the contrary, when the concentration of AFB₁ is low, the SA-HRP fixed on the magnetic particles will increase, and the detected chemiluminescence intensity will also increase. In theory, the chemiluminescence intensity is inversely proportional to the concentration of AFB₁.

3.2. Sensor Workflow

This design uses a self-made fiber optic sensor to detect the chemiluminescence intensity of the AFB₁ solution at different concentrations. The sensor system includes an optical signal input module, signal conversion module, filtering circuit, signal amplification circuit, and upper computer software in the computer. The circuit workflow diagram is shown in Figure 2.

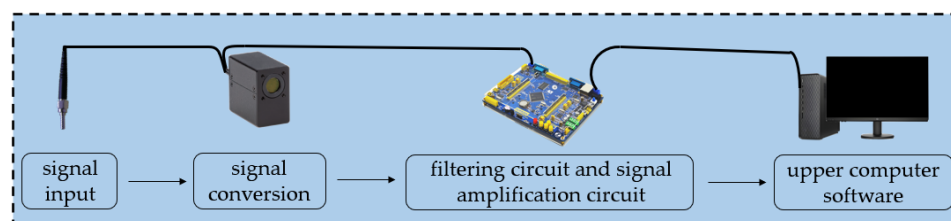


Figure 2. Sensor workflow diagram.

The optical signal input module, also known as optical fiber, transmits the detected chemiluminescence signal to the signal input module. The signal input module includes a photon counter and a microcontroller. The photon counter converts the number of detected photons into an equal number of standard TTL (Transistor–Transistor Logic) signals and outputs them to the microcontroller. The microcontroller counts the standard TTL signals and outputs the number of photons, which is the chemiluminescence intensity generated in the experiment. After passing through the circuit and signal amplification circuit, the data are finally transmitted to the computer.

To avoid errors caused by natural light, the experiment needs to be conducted in a dark room. And due to the lack of transparency of magnetic particles themselves, the detected chemiluminescence intensity may be slightly weakened compared to conventional methods, which needs to be considered when processing data. Moreover, the uneven concentration of magnetic particles at different positions in the solution can easily cause errors during detection, and it is necessary to control the errors by controlling the concentration of magnetic particles by centrifuging and mixing. The results detected by the light intensity detection equipment show that before the experiment, the number of photons in the darkroom was within 100. When the AFB₁ concentration was 0 ng/mL, the number of photons remained stable at around 40,000. When the AFB₁ concentration was 10 ng/mL, the number of photons remained stable at around 4500. Based on these data, errors can be minimized to the greatest extent possible.

3.3. Assessment of Detection Performance for Different Coating Modes

To verify the detection accuracy of the sensor for AFB₁ at concentrations of 0, 0.1, 0.3, 1, 3, and 10 ng/mL under different conditions of magnetic particles and microplates, this study conducted two sets of experiments with coated antigens on microplates and magnetic particles, respectively. The sensor detection curve shows that coating the antigen on a microplate resulted in higher chemiluminescence intensity, but the linear curve between chemiluminescence intensity and toxin concentration fluctuated more and had lower accuracy compared to the latter. Coating the antigen onto magnetic particles resulted in a certain degree of decrease in chemiluminescence intensity, but the linear curve showed better stability and accuracy. The specific data are shown in Figure 3.

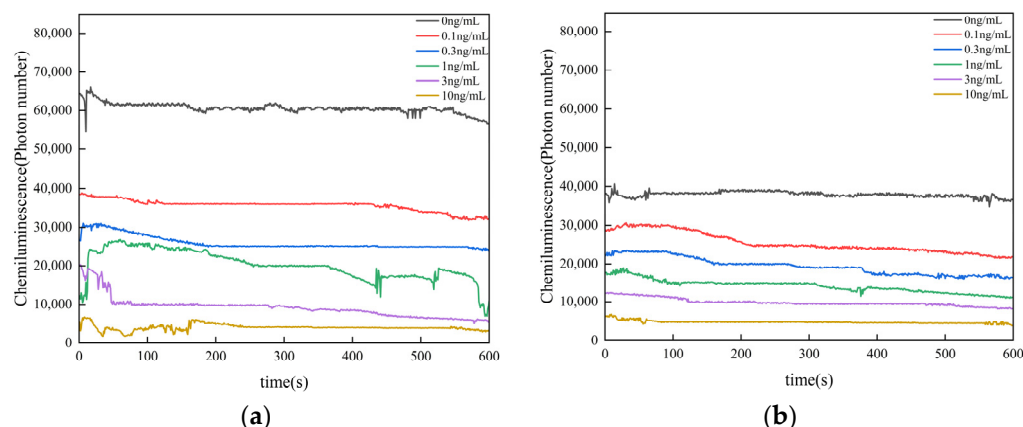


Figure 3. AFB₁ detection curve (a) with coated antigens on microplate and (b) AFB₁ detection curve with coated antigens on magnetic particles.

3.4. Optimization of Experimental Conditions

The concentration of the aptamer, concentration of the coated antigen, and pH value will affect the sensitivity of the detection system. To select the optimal concentration of aptamer and coated antigen, we conducted a checkboard titration experiment. The data are shown in Figure 4a. The experiment was conducted with concentrations of AFB₁-OVA of 0.1 µg/mL, 0.25 µg/mL, 0.5 µg/mL, and 1 µg/mL, and the corresponding concentrations of aptamer were 0.2, 0.4, 0.6, 0.8, and 1 nM, respectively. The AFB₁ concentration of control sample B_0 was 10 ng/mL, and the sensitivity of the sensor was calculated by B/B_0 . The test result of B/B_0 was 1.005, so the sensor obtained the most accurate experimental data when the aptamer concentration was 0.6 nM and the coated AFB₁-OVA concentration was 0.25 µg/mL. Consequently, 0.6 nM was determined as the optimal aptamer concentration, and 0.25 µg/mL was determined as the optimal concentration of coated AFB₁-OVA.

The optimal concentrations of luminol and H₂O₂ were determined when the concentration of magnetic particles was 10 µg/mL; the data are shown in Figure 4b. The concentrations of H₂O₂ were 0.5, 1.0, 1.5, 2, and 2.5 nM, and the corresponding concentrations of luminol were 0.5, 1.0, 1.5, 2, and 2.5 nM, respectively. The data in Figure 4b show that the highest chemiluminescence intensity was obtained by the sensor at both luminol and hydrogen peroxide concentrations of 2 nM.

The pH value of the aptamer solution is a key parameter, potentially resulting in the instability of the sensor, so we utilized different pH environments in the step of ligand binding to AFB₁, as shown in Figure 5. As the pH value (pH = 5, 6, 7, 8, and 9) of the aptamer solution increased, there was no significant change in the chemiluminescence intensity. This proves the acid and alkali resistance of the aptamer. Due to the relatively highest chemiluminescence intensity at pH value = 7, we ultimately chose to adjust the pH value to 7.0.

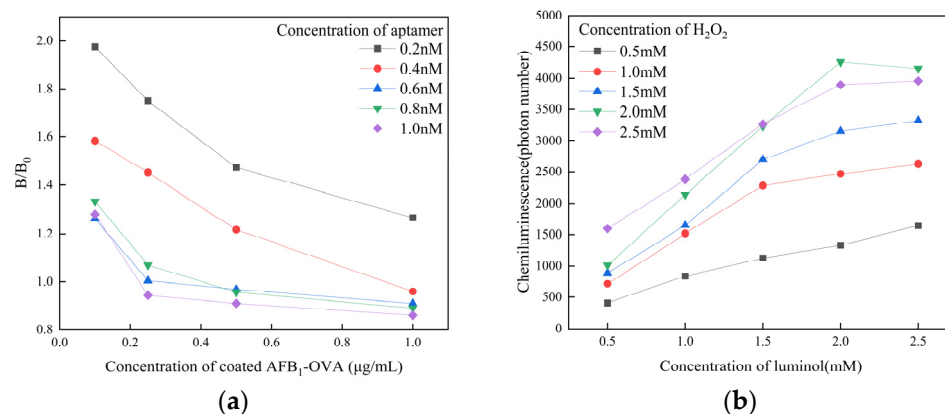


Figure 4. (a) The selection of concentration of AFB₁-OVA and aptamer and (b) the selection of concentration of H₂O₂ and luminol.

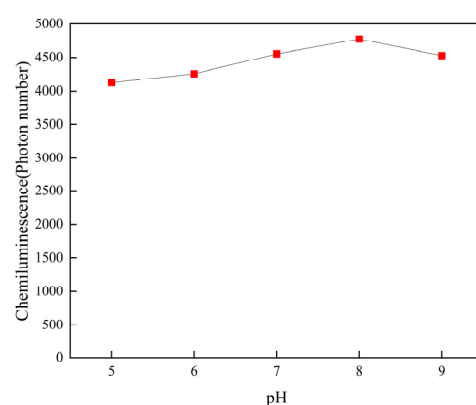


Figure 5. Effects of pH.

3.5. Detection of AFB₁ by the Aptamer Sensor

To verify the performance of the sensor under the two different coating conditions of microplate and magnetic particle, we used sensor tests in both situations. The chemiluminescence intensity of the antigen coated on microplate is shown in Figure 6a, and the chemiluminescence intensity of the antigen coated on magnetic particles is shown in Figure 6b. The chemiluminescence intensity under both coating conditions exhibited a notable decrease with an increasing AFB₁ concentration within the range of 0.1–10 ng/mL. The dynamic curves obtained under the condition with coated antigen on magnetic particles showed higher consistency than those obtained with coated antigen on microplate. And coating the antigen on magnetic particles resulted in a higher R-squared value; the curve equation for coated antigen on microplate is as follows:

$$y = 20,261.5 - 7010.7 \ln x, R^2 = 0.983,$$

The curve equation for coated antigen on magnetic particles is as follows:

$$y = 14,501.3 - 4434.1 \ln x, R^2 = 0.995.$$

The above results demonstrate that coating antigens on magnetic particles shows a better detection performance.

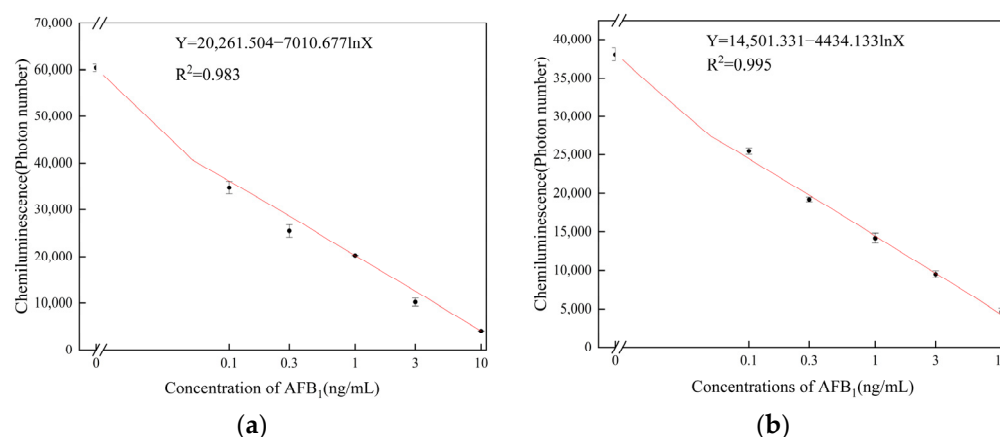


Figure 6. Sensor fitting curve diagram at different concentrations of AFB₁ (a) with coated antigen on microplate and (b) with coated antigen on magnetic particles.

3.6. Sensor Specificity and Anti-Interference

In order to investigate the specificity and anti-interference of the sensor, under the same conditions, a methanol/water (10:90, *v/v*) solution without AFB₁ content was used as the negative sample in the specificity and anti-interference ability tests of the sensor, and several common fungal toxins were introduced: AFB₂, AFG₁, and OTA were used as positive samples, and 100 μ L of the above fungal toxin solutions with a concentration of 10 ng/mL were taken for detection. We assumed that the number of photons detected from the negative sample was X_F , and the number of photons detected from the positive sample was X_P ; the inhibition ratio was $I = X_P / X_F$; the sensor specificity detection results are shown in Figure 7a. The sensor had the lowest inhibition ratio for AFB₁, and there was no significant response to other fungal toxins; this proves that the sensor has good specificity for AFB₁.

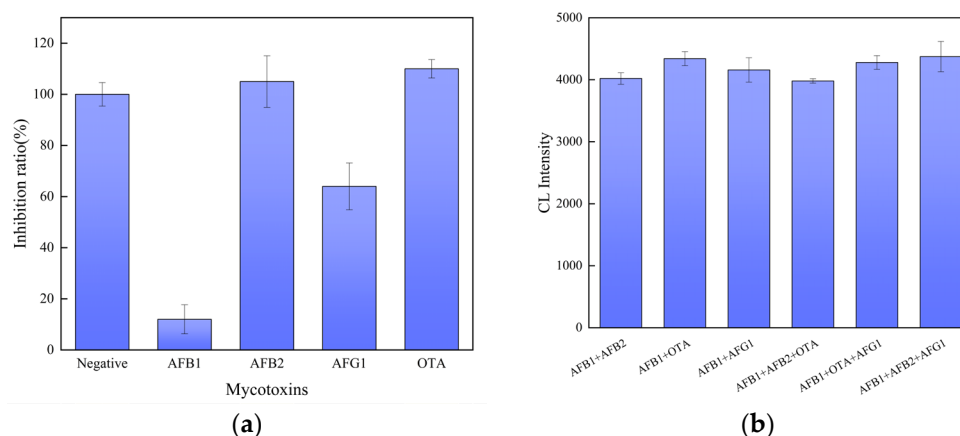


Figure 7. Inhibition ratio (a) and the chemiluminescence intensity of the sensor to AFB₁, AFB₂, AFB₁ + AFB₂, AFG₁, and AFB₁ + AFG₁ (b) ($n = 3$).

The anti-interference ability of the prepared sensor was also crucial for assessing its performance. After mixing the AFB₁ solution with equal amounts of the solution of other fungal toxins, we used sensors to detect the mixed solutions. The detected chemiluminescence intensity of the mixed solution showed the anti-interference ability of the sensor. The anti-interference detection results are shown in Figure 7b, and the chemiluminescence intensity of the sensor to different mixed solutions was basically similar, which proves that the sensor has good anti-interference ability.

3.7. Application of Sensor in Wheat Samples

To further validate the application and feasibility of the sensor for AFB₁ detection, we prepared the spiked wheat sample using a previously established method [27,28]. According to Table 1, using spiked wheat samples with AFB₁ concentrations of 0, 0.5, 1, 2, 5, and 10 µg/kg as the negative sample, the spiked recovery rate of AFB₁ in the wheat sample solution was 79.19% to 113.21%, indicating that the aptamer sensor could be employed for AFB₁ detection in wheat samples.

Table 1. Determination of recovery of AFB₁ in wheat samples (n = 3).

Added AFB ₁ /(µg/kg)	Found AFB ₁ /(µg/kg)	Recovery/%
0	<LOD	-
0.5	0.396 ± 0.050	79.19 ± 10.01
1	0.985 ± 0.127	98.53 ± 12.69
2	2.264 ± 0.106	113.21 ± 5.31
5	4.628 ± 0.351	92.56 ± 7.02
10	10.929 ± 0.429	109.29 ± 4.29

3.8. Comparison of the Chemiluminescence Aptamer Sensor

Before this study, there were many sensors using aptamer or chemiluminescence methods to detect AFB₁, and several relevant studies about chemiluminescence assays or aptamer assays are listed in Table 2. Compared to the method using chemiluminescence for AFB₁ detection, this study yielded a lower detection limit and similar detection range. Compared to our study, sensors using electrochemical and fluorescence methods have a wider detection range, but their detection limits and ranges are lower than those of our design. And compared with other methods in Table 2, the material price of this design is lower, and the manufacturing method is simpler.

Table 2. Comparison of the related chemiluminescence aptamer sensor.

Methods	LOD	Linear (L)/Dynamic (D) Range	Tested Samples	Reference
Chemiluminescence Aptamer	0.09 ng/mL	(D) 0.1–10 ng/mL	Wheat	This work
Chemiluminescence Aptamer	0.20 ng/mL	(L) 0.5–40 ng/mL	Peanut and milk	[25]
Chemiluminescence Antibody	0.53 ng/mL	(D) 0.1–10 ng/mL	Wheat	[31]
Fluorescent Aptamer	1.6 ng/mL	(L) 5–100 ng/mL	Rice cereal	[32]
Fluorescent Aptamer	0.35 ng/mL	(L) 0–180 ng/mL	Corn, milk, and rice	[33]
Fluorescent Aptamer	0.62 ng/mL	(D) 0.62–312.27 ng/mL	Serum, urine, wine, and beer	[34]
Electrochemiluminescence Aptamer	0.17 ng/mL	(L) 0.50–200.00 ng/mL	Corn	[35]

4. Conclusions

In this study, we developed a chemiluminescence indirect competitive aptamer sensor for aflatoxin B₁ (AFB₁) utilizing aptamer-linked streptavidin–horseradish peroxidase (SA-HRP), and we applied the sensor to wheat samples. The sensor is capable of specifically recognizing AFB₁ and accurately measuring its concentration. It operates on the principle that AFB₁ and AFB₁ antigens compete for binding to the aptamer, with the chemiluminescence intensity detected through a custom-built chemiluminescence detection device. The high specificity and binding efficiency of the aptamer for AFB₁ were confirmed through both simulations and experimental validations. The results indicated that the change in chemiluminescence intensity is linear within the concentration range of 0.1–10 ng/mL. For wheat samples spiked with AFB₁ at a concentration of 10 ng/mL, the recovery rate after three repeated detections ranged from 79.19% to 113.21%. Compared to other sensors, this

design features a low cost and a straightforward manufacturing process. Additionally, the experimental results demonstrate that this sensor exhibits high accuracy and a low detection limit. This study holds innovative significance for the advancement of low-cost and high-sensitivity AFB₁ detection equipment.

Author Contributions: Conceptualization, Z.Z. (Zebing Zhang); methodology, C.W.; writing—review and editing, Z.Z. (Zebing Zhang) and Z.Z. (Zhike Zhao); experiment, Z.Z. (Zebing Zhang); writing—original draft preparation, Z.Z. (Zebing Zhang); funding acquisition, Z.Z. (Zhike Zhao). All authors have read and agreed to the published version of the manuscript.

Funding: This work was co-sponsored by the Collaborative Innovation Project of Natural Science Project of Zhengzhou Science and Technology Bureau (22ZZRDZX07).

Institutional Review Board Statement: Not applicable.

Informed Consent Statement: Not applicable.

Data Availability Statement: The data presented in this study are available on request from the corresponding authors.

Conflicts of Interest: The authors declare no conflicts of interest.

References

1. Mao, L.; Liu, H.; Yao, L.; Wen, W.; Chen, M.-M.; Zhang, X.; Wang, S. Construction of a dual-functional CuO/BiOCl heterojunction for high-efficiently photoelectrochemical biosensing and photoelectrocatalytic degradation of aflatoxin B1. *Chem. Eng. J.* **2022**, *429*, 132297. [\[CrossRef\]](#)
2. Shephard, S.G. Determination of mycotoxins in human foods. *Chem. Soc. Rev.* **2008**, *37*, 2468–2477. [\[CrossRef\]](#)
3. Wu, H.; Wang, H.; Wu, J.; Han, G.; Liu, Y.; Zou, P. A novel fluorescent aptasensor based on exonuclease-assisted triple recycling amplification for sensitive and label-free detection of aflatoxin B1. *J. Hazard. Mater.* **2021**, *415*, 125584. [\[CrossRef\]](#)
4. Kong, Y.; Zhu, Y.; Song, J.; Liu, Q.; Song, L.; Fei, X.; Li, X. A novel multimode biosensor for sensitive detection of AFB1 in food based on Mxenes nano enzymes. *Food Chem.* **2023**, *426*, 136645. [\[CrossRef\]](#)
5. Han, W.; Li, Y.; Gao, G.; Zhang, X. Application of Aptamer Biosensor in Detection of Aflatoxin B1. *Fenxi Ceshi Xuebao (J. Instrum. Anal.)* **2023**, *42*, 368–374.
6. Zheng, M. Construction of Aflatoxin B1 Smart Hydrogel Detection Sensor and Screening of Its Precursor Aptamer. Master's Thesis, Henan University of Technology, Zhengzhou, China, 2023.
7. Nataša, H.; Martina, M.; Dušan, Ž.; Janez, K.; Andrea, J.; Aaron, D.; James, L.; Walsh, U. Cold atmospheric pressure plasma-assisted removal of aflatoxin B1 from contaminated corn kernels. *Plasma Process. Polym.* **2020**, *18*, 2000163.
8. Ma, H.; Yuan, Z.; Liu, J.; Zhang, X. Research on the harmful effect of aflatoxin B1 on animals. *Chin. Livest. Poult. Breed.* **2022**, *18*, 3–8.
9. Gao, Y.; Su, J. Research Progress on the effect of related metabolic enzymes on the metabolism of aflatoxin B1 (AFB1). *World J. Tumor* **2007**, *6*, 277–281+299.
10. GB 2761-2017; National Food Safety Standards, Limit of Fungal Toxins in Food. National Health and Family Planning Commission of the PRC, China Food and Drug Administration: Beijing, China, 2017.
11. Xuan, Z.; Liu, H.; Ye, J.; Li, L.; Tian, W.; Wang, S. Reliable and disposable quantum dot-based electrochemical immunosensor for aflatoxin B1 simplified analysis with automated magneto-controlled pretreatment system. *Anal. Bioanal. Chem.* **2020**, *412*, 7615–7625. [\[CrossRef\]](#)
12. Zheng, M.; Liu, H.; Ye, J.; Ni, B.; Xie, Y.; Wang, S. Target-responsive aptamer-cross-linked hydrogel sensors for the visual quantitative detection of aflatoxin B1 using exonuclease I-Triggered target cyclic amplification. *Food Chem. X* **2022**, *15*, 100395. [\[CrossRef\]](#)
13. Daradimos, E.; Marcaki, P.; Koupparis, M. Evaluation and validation of two fluorometric HPLC methods for the determination of aflatoxin B1 in olive oil. *Food Addit. Contam.* **2000**, *17*, 65–73. [\[CrossRef\]](#)
14. Wu, H.; Wu, J.; Liu, Y.; Wang, H.; Zou, P. Target-triggered and T7 exonuclease-assisted cascade recycling amplification strategy for label-free and ultrasensitive fluorescence detection of aflatoxin B1. *Sens. Actuators B Chem.* **2020**, *321*, 128599. [\[CrossRef\]](#)
15. Yan, C.; Yang, L.; Yao, L.; Xu, J.; Yao, B.; Liu, G.; Chen, W. Ingenious electrochemiluminescence bioaptasensor based on synergistic effects and enzyme-driven programmable 3D DNA nanoflowers for ultrasensitive detection of aflatoxin B1. *Anal. Chem.* **2020**, *92*, 14122–14129. [\[CrossRef\]](#)
16. Mao, L.; Xue, X.; Xu, X.; Wen, W.; Chen, M.M.; Zhang, X.; Wang, S. Heterostructured CuO-g-C₃N₄ nanocomposites as a highly efficient photocathode for photoelectrochemical aflatoxin B1 sensing. *Sens. Actuators B Chem.* **2021**, *329*, 129146. [\[CrossRef\]](#)

17. He, H.; Sun, D.W.; Pu, H.; Huang, L. Bridging Fe₃O₄@ Au nanoflowers and Au@ Ag nanospheres with aptamer for ultrasensitive SERS detection of aflatoxin B1. *Food Chem.* **2020**, *324*, 126832. [\[CrossRef\]](#)
18. Liu, X.; Singh, R.; Li, M.; Li, G.; Min, R.; Marques, C.; Zhang, B.; Kumar, S. Plasmonic Sensor Based on Offset-Splicing and Waist-Expanded Taper Using Multicore Fiber for Detection of Aflatoxins B1 in Critical Sectors. *Opt. Express* **2023**, *31*, 4783–4802. [\[CrossRef\]](#)
19. Huang, X.; Chen, Y.; Wang, J.; Song, L. Research progress of aptasensors for the detection of aflatoxins. *Food Ferment. Ind.* **2024**, *50*, 323–331.
20. Ruscito, A.; DeRosa, M. Small-molecule binding aptamers: Selection strategies, characterization, and applications. *Front. Chem.* **2016**, *4*, 14. [\[CrossRef\]](#)
21. Zhu, Z.; Song, Y.; Li, C.; Zou, Y.; Zhu, L.; An, Y.; Yang, C.J. Monoclonal surface display SELEX for simple, rapid, efficient, and cost-effective aptamer enrichment and identification. *Anal. Chem.* **2014**, *86*, 5881–5888. [\[CrossRef\]](#)
22. Zhao, F.; Zhang, Y.; Liu, T.; Han, M.; Wu, Y. Progress on Detection Method of AFB1 in Cereal and Application of Aptamer. *Mod. Agric. Sci. Technol.* **2024**, *13*, 153–156. [\[CrossRef\]](#)
23. Li, H.; He, Z. Magnetic particle-based DNA hybridization assay with chemiluminescence and chemiluminescent imaging detection. *Analyst* **2009**, *134*, 800–804. [\[CrossRef\]](#)
24. Shim, W.; Mun, H.; Joung, H.; Ofori, J.; Chung, D.; Kim, G. Chemiluminescence competitive aptamer assay for the detection of aflatoxin B1 in corn samples. *Food Control* **2014**, *36*, 30–35. [\[CrossRef\]](#)
25. Yao, Y.; Wang, H.; Wang, X.; Wang, X.; Li, F. Development of a chemiluminescent aptasensor for ultrasensitive and selective detection of aflatoxin B1 in peanut and milk. *Talanta* **2019**, *201*, 52–57. [\[CrossRef\]](#)
26. Hu, L.; Wu, C.; Zhao, Z.; Xu, K. Design of optical fiber detection system for aflatoxin B1. *Electron. Meas. Technol.* **2022**, *45*, 39–44.
27. Lu, R.; Chen, R.; Ren, S.; Gao, Z.; Liang, J. Detection of aflatoxin B1 in vegetable protein meat based on surface enhanced Raman spectral aptamer sensor. *J. Food Saf. Qual.* **2023**, *14*, 1–9.
28. Wang, J.; Li, S.; Wei, J.; Jiao, T.; Chen, Q.; Oyama, M.; Chen, Q.; Chen, X. Screening-capture-integrated Electrochemiluminescent aptasensor based on mesoporous silica nanochannels for the ultrasensitive detection of deoxynivalenol in wheat. *J. Agric. Food Chem.* **2023**, *71*, 12052–12060. [\[CrossRef\]](#)
29. Fan, Y.; Wu, C.; Zhao, Z. Quantitative determination of aflatoxin B1 in wheat by quantum dot fluorescence microsphere immunoassay. *J. Food Saf. Qual.* **2024**, *15*, 208–216.
30. Kong, W. Preparation and Analytical Application of Chemiluminescence Functionalized Magnetic Microbeads and Study on Single Particle Chemiluminescence Imaging. Ph.D. Thesis, University of Chinese Academy of Sciences, Beijing, China, 2019.
31. Wang, J.; Wu, C. Plastic Optical Fiber Functionalized with Polyaniline for the Detection of Aflatoxin B1 Concentration. *Semiconductroptoelectronics* **2024**, *45*, 111–116.
32. Chen, L.; Wen, F.; Li, M.; Guo, X.; Li, S.; Zheng, N.; Wang, J. A simple aptamer-based fluorescent assay for the detection of Aflatoxin B1 in infant rice cereal. *Food Chem.* **2017**, *215*, 377–382. [\[CrossRef\]](#)
33. Jia, Y.; Zhou, G.; Wang, X.; Zhang, Y.; Li, Z.; Liu, P.; Zhang, J. A metal-organic framework/aptamer system as a fluorescent biosensor for determination of aflatoxin B1 in food samples. *Talanta* **2020**, *219*, 121342. [\[CrossRef\]](#)
34. Jia, Y.; Zhang, X.; Kuang, X.; Fan, D.; Sun, X.; Ren, X.; Wei, Q. 1, 1, 2, 2-tetra (4-carboxylphenyl) ethylene-based metal-organic gel as aggregation-induced electrochemiluminescence emitter for the detection of aflatoxin B1 based on nanosurface energy transfer. *Anal. Chem.* **2024**, *96*, 12593–12597. [\[CrossRef\]](#)
35. Sun, L.; Zhao, Q. Direct fluorescence anisotropy approach for aflatoxin B1 detection and affinity binding study by using single tetramethylrhodamine labeled aptamer. *Talanta* **2018**, *189*, 442–450. [\[CrossRef\]](#)

Disclaimer/Publisher's Note: The statements, opinions and data contained in all publications are solely those of the individual author(s) and contributor(s) and not of MDPI and/or the editor(s). MDPI and/or the editor(s) disclaim responsibility for any injury to people or property resulting from any ideas, methods, instructions or products referred to in the content.